



## Evaluation of the cooling potential of a vertical greenery system coupled to a building through an experimentally validated transient model

Maurizio Detommaso <sup>a</sup>, Vincenzo Costanzo <sup>a,\*</sup>, Francesco Nocera <sup>a</sup>, Gianpiero Evola <sup>b</sup>

<sup>a</sup> Department of Civil Engineering and Architecture, University of Catania, Via Santa Sofia 64, 95125, Catania, Italy

<sup>b</sup> Department of Electric, Electronic and Computer Engineering, University of Catania, Via Santa Sofia 64, 95125, Catania, Italy

### ARTICLE INFO

#### Keywords:

Green façade

Vertical greenery system

Experimental measurements

TRNSYS

Mediterranean climate

### ABSTRACT

Despite several studies showed that Vertical Greenery Systems (VGSS) have relevant thermal benefits at urban and building scales, researches devoted to investigate the benefits of a green facade through detailed transient thermal simulations are scarce. Furthermore, a study comparing the effectiveness of different plant types is still missing. The present paper aims to fill such gaps by studying the effectiveness of a green façade to improve the thermal behaviour of a well-insulated lightweight building in the Mediterranean area, as well as the perceived indoor thermal conditions, based on both on-site experimental measurements and dynamic thermal simulations with a novel Type in TRNSYS validated through the monitoring campaign. To this aim, two identical full-scale prefabricated modules were installed and monitored at the University Campus of Catania (Italy), differing from each other because one of them hosted a climbing plant species in its west façade. The validated numerical model was then used to appraise the cooling effect of the green façade with two different plant species commonly used in Mediterranean countries (*Trachelospermum Jasminoides* and *Hedera Helix* namely). Results show that *Hedera helix* ensures the best performance when the foliage layer is at an intermediate state of its growing process, while under full foliage development the species investigated show almost the same performance. The incoming heat flux can be strongly attenuated, showing a quite flat daily profile, while the peak value of the internal and external surface temperature of the wall can be reduced by up to 1.6 °C and 10.5 °C, respectively.

### 1. Introduction

The urbanization process has led to a significant reduction in the extension of green spaces and to an increasing amount of paved areas and buildings with low albedo [1–4]. The lack of green infrastructures and the presence of low-albedo materials are two main causes of the Urban Heat Island (UHI) phenomenon [3,4], with consequent adverse effects on human and socio-economic development such as increased pedestrian thermal discomfort and related health problems, increased energy needs for space cooling in buildings, biodiversity decline and atmospheric pollution [5–10].

In this context, Urban Green Infrastructures such as trees, green roofs and Vertical Greenery Systems (VGSS) can provide multiple ecosystem services at both building and urban scale [11,12]. Among the available greenery strategies, VGSS have great potential at building scale because the wall surfaces may become more relevant than roof surfaces in terms of heat exchange in dense built-up urban areas [13,14].

On the one hand, at a city scale, VGSS are able to mitigate the urban

heat island effect by decreasing the outdoor air temperature [15–17], thus contributing to improve outdoor thermal comfort of city dwellers [18]. The vegetation can attenuate the heat stress providing shading and evaporative cooling effects, thanks to their photosynthesis and transpiration processes [19]. In terms of social and aesthetic benefits, VGSS improve the city image, the lifestyle of residents, and increase the architectural value of the urban settlements [20,21]. On the other hand, at a building scale, VGSS can mitigate heat transfer with the outdoors and reduce the cooling load, thanks to the shade, evaporation, and transpiration of the foliage layer [22,23].

According to the different growing methods and construction techniques, VGSS are classified into Green Façades (GFs) and Living Walls Systems (LWSs), also known as Green Walls (GWs) [13,19,22,24–26]. Traditional Green Façades are considered a direct greenery system, consisting of climbing plants attached directly to the building and rooted in the ground [13,19,24,27,28]. Instead, indirect green façades rely on a vertical support structure for climbing plants development; the structure can be composed of cables, mesh or trellis made with aluminum, plastic,

\* Corresponding author.

E-mail address: [vincenzo.costanzo@unict.it](mailto:vincenzo.costanzo@unict.it) (V. Costanzo).

wood, and steel. Unlike Green Façades, Living Walls Systems have the growing media embedded in the building wall, and include materials and technologies supporting more typologies of plants to form a uniform growth along the wall [19,26,29].

Although several studies have investigated the effectiveness of indirect green facades to reduce the energy consumption at building scale, only few authors reported experimental and simulated data in the Mediterranean climate [13,22,24,30–33]. Most of these studies dealt with the experimental investigation on existing buildings, building prototypes or laboratory test rooms [13,22,24,30], predominantly carried out on façades made with concrete, brick, and hollow clay blocks [30,34] and covered by specific perennial and evergreen species such as ivy (*Hedera Helix*, *Parthenocissus Tricuspidata*) [30]. On the contrary, a lack of studies regarding green facades on lightweight and well-insulated buildings has been observed [30,35], in spite of the relevance of this building typology as temporary constructions for, e.g., post-disaster events or construction works.

Besides, it is worth pointing out that there is a shortage of studies where transient thermal simulations couple the thermal behavior of a building with the thermal performance of the green façades they are equipped with. This is mainly due to the lack of analytical models and calculation codes able to comprehensively account for the complexity of the physical phenomena involving the plants and their interaction with a building [36]. In fact, most recent studies are based on the experimental monitoring of the internal and external surface temperature of a wall equipped with a green façade, and of the outdoor air temperature adjacent to the vertical greenery layer [37]. Only few studies accounted for indoor air temperature in order to assess the indoor thermal conditions determined by the presence of VGSs, and most of them were carried out in Europe and Asia during the warmest periods of the year [30,37].

The present paper aims to fill this gap within the current literature through the detailed dynamic simulation of the cooling effect of an indirect green façade applied to a well-insulated lightweight building in

the Mediterranean area. First, an experimental monitoring campaign verified the internal and external surface temperature – along with the indoor air temperature – of two mock-ups equipped either with a green façade or a bare wall, respectively, on their west-facing façade (the orientation suffering the most from overheating at this latitude). The monitoring results were then used to calibrate and validate a TRNSYS model where the building is coupled to a dedicated Type for transient simulations of VGS, which was finally run to estimate the possible improvements achievable in terms of temperature decrease and heat flux reduction through the wall thanks to different plant species commonly used in Mediterranean countries at different growth stages.

## 2. Previous studies about the thermal performance of green facades in warm climates

The main studies about the thermal performance of an indirect green façade carried out in the warm areas of Mediterranean climate [12,22,35,38–40], in humid-tropical regions [41–44] and in very hot dry zone [45], are summarized in Table 1. The table reports, for each study, the plant species installed on the green facade, the adopted methodology (experimental and/or numerical), the thermo-physical parameters used to describe the cooling thermal performance, the location of the case study, and the main results. As it is possible to observe from Table 1, the external surface temperature ( $T_{os}$ ), internal surface temperature ( $T_{is}$ ), indoor air temperature ( $T_a$ ) and heat flux exchanged through the wall ( $Q$ ) were the parameters mainly investigated. Consequently, the main results are presented in terms of reduction of these parameters in the peak hours of the hottest days, obtained with a green façade in comparison with a bare wall and indicated as “ $\Delta T_{os}$ ”, “ $\Delta T_{is}$ ”, “ $\Delta T_a$ ”, and “ $\Delta Q$ ” respectively. Furthermore, “N”, “E”, “S”, and “W” indicate the North, East, South and West orientation.

Most studies have considered a vertical vegetation layer installed on a heavy wall (made with concrete or bricks), and are based on experimental measurements typically carried out during the summer [12,35,

**Table 1**  
Previous researches about the thermal performance of an indirect green façade in warm climates under free-running conditions.

| Year   | Author                    | Plant species  | Plant typology | Back wall structure                  | Parameter                     | Location                   | Main results  |
|--|---------------------------|--|----------------|--------------------------------------|-------------------------------|----------------------------|---|
| <i>Experimental measurements</i>                           |                           |  |                |                                      |                               |                            |   |
| 2014   | Coma et al. [12]          | <i>Parthenocissus Tricuspidata</i>                               | Deciduous      | Alveolar bricks                      | $T_{os}$<br>$T_{is}$<br>$T_a$ | Puigverd De Leida (Spain)  | $\Delta T_{os} = 14.0 \text{ }^{\circ}\text{C}$<br>$\Delta T_{is} = 0.5 \div 2.0 \text{ }^{\circ}\text{C}$<br>$\Delta T_a = 1.0 \text{ }^{\circ}\text{C}$<br>$\Delta T_{os} = 9.0 \text{ }^{\circ}\text{C}$ |
| 2018   | Vox et al. [35]           | <i>Rhynchospermum Jasminoides</i><br><i>Pandorea Jasminoides</i> | Evergreen      | Perforated bricks                    | $T_{os}$                      | Bari (Italy)               |   |
| 2017   | Perez et al. [38]         | <i>Parthenocissus Tricuspidata</i>                               | Deciduous      | Alveolar bricks                      | $T_{os}$                      | Puigverd De Leida (Spain)  | E: $\Delta T_{os} = 16.0 \text{ }^{\circ}\text{C}$<br>S: $\Delta T_{os} = 15.0 \text{ }^{\circ}\text{C}$<br>W: $\Delta T_{os} = 16.0 \text{ }^{\circ}\text{C}$  |
| 2022   | Campiotti et al. [39]     | <i>Parthenocissus quinquefolia</i>                               | Deciduous      | Hollow bricks with air gap           | $T_{os}$                      | Rome (Italy)               | $\Delta T_{os} = 15.0 \text{ }^{\circ}\text{C}$   |
| 2019   | Zhang et al. [41]         | <i>Pyrostegia venusta</i>  | Evergreen      | Lime sand bricks                     | $T_{os}$<br>$T_a$             | Guangzhou (Southern China) | W: $\Delta T_{os} = 14.0 \text{ }^{\circ}\text{C}$<br>$\Delta T_a = 1.5 \text{ }^{\circ}\text{C}$   |
| 2019   | Peng et al. [42]          | <i>Hedera Helix</i>  | Evergreen      | Concrete bricks                      | $T_{os}$<br>$T_a$             | Dujiangyang (China)        | $\Delta T_{os} = 13.9 \text{ }^{\circ}\text{C}$<br>$\Delta T_a = 1.8 \text{ }^{\circ}\text{C}$  |
| 2019   | Kokogiannakis et al. [43] | <i>Philodendron scandens</i>                                     | Evergreen      | Lightweight bricks                   | $T_{os}$                      | Ningbo (East China)        | $\Delta T_{os} = 11.0 \text{ }^{\circ}\text{C}$   |
| 2019   | Nguyen et al. [44]        | <i>Bougainvillea</i>   | Evergreen      | Lightweight bricks                   | $T_a$                         | Hanoi (Vietnam)            | $\Delta T_a = 1.0 \text{ }^{\circ}\text{C}$   |
| <i>Numerical simulations</i>                               |                           |  |                |                                      |                               |                            |   |
| 2020   | Niki-Assimakopoulos [22]  | <i>Hedera Helix</i>  | Evergreen      | Brick                                | $Q$<br>$T_{os}$               | (Greece)                   | $\Delta T_{os} = 11.0 \text{ }^{\circ}\text{C}$   |
| 2023   | Banti et al. [40]         | Comparison of different species                                  | Deciduous      | Precast concrete with EPS insulation | $Q$<br>$T_{os}$<br>$T_{is}$   | Tuscany (Italy)            | $\Delta Q = 2 \text{ kW}$<br>$\Delta T_{os} = 8.0 \text{ }^{\circ}\text{C}$<br>$\Delta T_{is} = 0.6 \text{ }^{\circ}\text{C}$   |
| <i>Experimental measurements and numerical simulations</i> |                           |  |                |                                      |                               |                            |   |
| 2022   | Freewan et al. [45]       | <i>Hedera Helix</i>  | Evergreen      | Precast concrete                     | $T_{os}$<br>$T_{is}$          | Irbid (Jordan)             | S: $\Delta T_{os} = 11.0 \text{ }^{\circ}\text{C}$<br>S: $\Delta T_{is} = 3.5 \text{ }^{\circ}\text{C}$   |

38–45]. All papers reported in Table 1 have investigated the effects of the green façade under indoor free-floating conditions; the most measured parameter is the external surface temperature of the wall behind the vegetation layer [12,35,38–45]. The only studies that dealt with the experimental evaluation of the internal surface temperature and indoor air temperature in a building equipped with indirect green facades in Mediterranean climates were carried out by Perez [38] and Coma et al. [12].

Regarding numerical studies, most analytical models of VGSs only consider plants as a conventional shading device without taking into account the evapotranspiration phenomena and other biophysical effects [37]. As an example, the DesignBuilder software tool allows to simulate the thermal performance of VGSs based on a simplified approach that accounts only for the shading effect of the greenery layer [40]. Based on this method, Banti et al. compared the results of dynamic simulations of an indirect green facade with the ones certified by experimental campaigns available in the literature, and with the findings provided by previous similar research [40]. Freewan et al. [45] validated the building simulation model by comparing the results of dynamic simulations and experimental measurements in terms of indoor air temperature.

Only a few mathematical models have been proposed for assessing the transient thermal performance of VGS, and one of the most comprehensive is that of Dahanayake et al. [37] who developed a transient model of VGS based on the heat balance principle of the foliage and substrate vertical layers to be integrated into the EnergyPlus software. Also Djedjig et al. [46] dealt with a similar heat balance model between the canopy and substrate layers, but this time to be integrated with the TRNSYS whole building software tool.

Unlike the studies of Dahanayake and Djedjig, who dealt with direct green facades modelling, this paper makes use of a novel VGF model [47] for indirect green facades modelling coupled to the multizone building model in TRNSYS.

### 3. Methodology

The investigation relies on a methodological approach consisting of the following phases:

1. Construction of two experimental mock-ups, one with and one without an indirect green façade;
2. Experimental measurement of indoor air temperature and internal surface temperature in both mock-ups for a typical summer week;
3. Creation of a detailed dynamic thermal model with the TRNSYS software tool;
4. Forcing of climate data input using locally measured weather data;
5. Calibration of the model by varying the most influential thermo-physical features of the vegetation layer in the green façade;
6. Validation of the model through statistical indices;
7. Assessment of the cooling effects of the most commonly used plant species in green facades in the European countries, namely *Trachelospermum Jasminoides* and *Hedera Helix*.

Fig. 1 summarizes the methodological workflow adopted in this research.

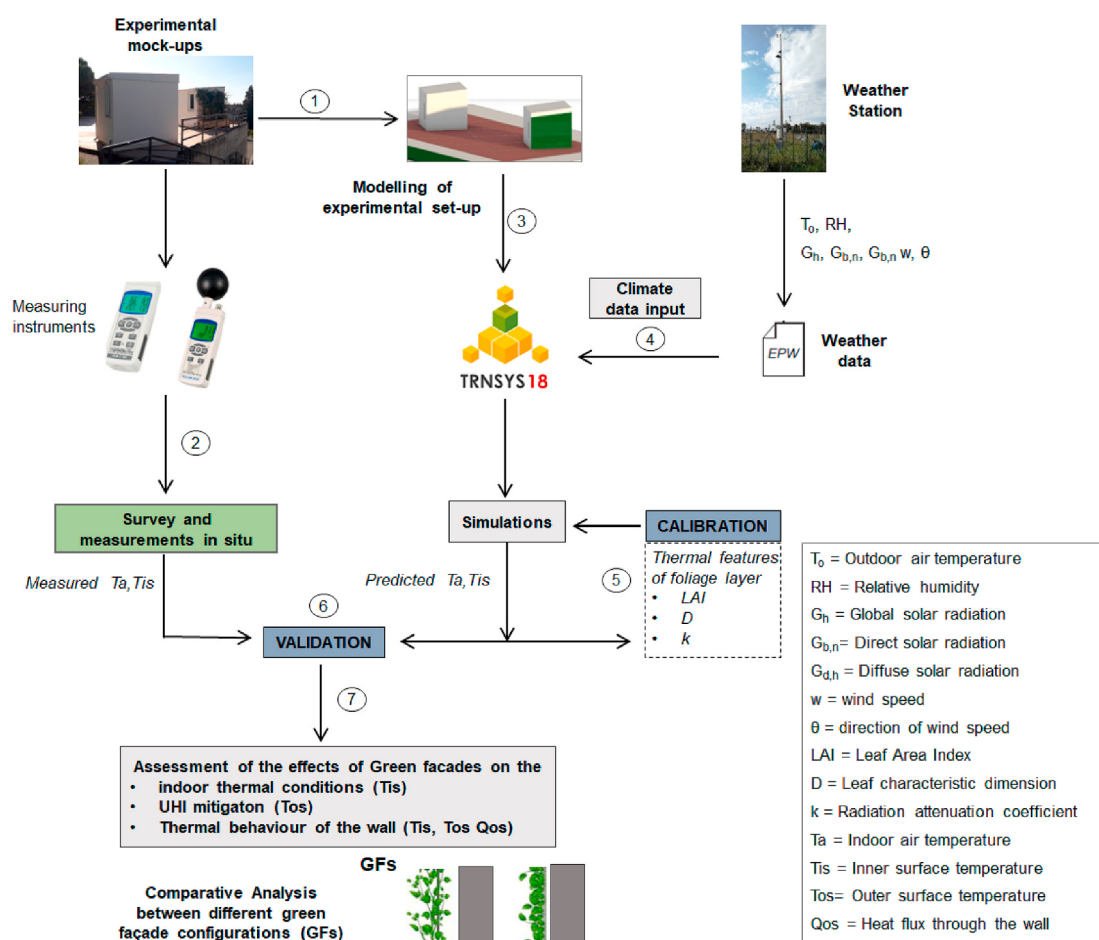


Fig. 1. Workflow of the research methodology.

### 3.1. Weather and experimental data collection

The weather data implemented in the TRNSYS model were taken from the PCE-FWS 20 N weather station placed on top of a building near the experimental site, in the University Campus of Catania, which records air temperature, relative humidity, wind speed and direction with a sampling time of 5 min [48]. The measurement range, accuracy, and other features of the sensors included in the weather station are reported in Table 2. Global, Direct and Diffuse solar irradiance values were instead taken from the weather station of the “Sicilian Agro-meteorological Informative Service” (SIAS), placed in the immediate surroundings of the city of Catania. In order to show the effects of the green façade, a typical summer week (from 8th to 14th July) was selected for the thermal analysis. The hourly values of outdoor air temperature ( $T_o$ ), relative humidity (RH), global horizontal irradiance ( $G_h$ ) and wind speed (w) recorded during this week are depicted in Fig. 2.

The validation of the thermal model built in TRNSYS has been accomplished by comparing the simulation outcomes with on-site experimental measurements carried out in the prefabricated modules with and without green façade, respectively. To this aim, indoor air temperature, relative humidity and internal surface temperature were detected at 10-min intervals. Air temperature and relative humidity were recorded using a PCE-WB 20SD multifunction thermometer, while surface temperature values were recorded by means of a multiple thermometer PCE-T390. The PCE-T390 multiple thermometer is equipped with four Pt-100 thermocouples, while the PCE-WB 20SD multifunction thermometer is equipped with air temperature and relative humidity sensor. The features of these devices are reported in Table 2. Both measuring devices were placed in the center of the experimental mock-ups at a height of 1.10 m above the floor. During the measurements, no activities were carried out indoors and no HVAC system was in operation, so that free-running conditions were realized; the measurement process complied with the suggestions of the ISO 7726 Standard [49].

### 3.2. Green façade thermal modelling in TRNSYS and validation of the model

The first attempts to include vertical greenery systems in building energy models only included the shading effect of vegetation, and their major drawback is that evapotranspiration was not considered [36]. In fact, this is a key effect that needs to be considered for a careful evaluation of the impact of green façades on the thermal performance of buildings [36,37]. Nevertheless, significant advances in the thermal

**Table 2**  
Technical features of the devices used in the experimental campaign.

| Device          | Sensor                        | Accuracy   | Resolution           | Measurement range               |
|-----------------|-------------------------------|--|----------------------|---------------------------------|
| PCE-FWS<br>20 N | Air temperature ( $T_a$ )     | $\pm 1^\circ\text{C}$  | 0.1 $^\circ\text{C}$ | -40 $\div$ +60 $^\circ\text{C}$ |
|                 | Relative humidity (RH)        | $\pm 4\%$ (range 20 $\div$ 80%)<br>$\pm 6\%$ otherwise                                   | 0.1%                 | 1 $\div$ 99%                    |
|                 | Wind speed (v)                | $\pm 1 \text{ m/s}$ (range 0 $\div$ 5 $\text{m/s}$ )<br>$\pm 10\%$ ( $> 5 \text{ m/s}$ ) | 0.1 $\text{m/s}$     | 0 $\div$ 50 $\text{m/s}$        |
| PCE-T390        | Surface Temperature ( $T_s$ ) | $\pm (0.4\% + 0.5^\circ\text{C})$  | 0.1 $^\circ\text{C}$ | -50 $\div$ 999 $^\circ\text{C}$ |
| PCE-WB<br>20SD  | Air temperature ( $T_a$ )     | $\pm 0.8^\circ\text{C}$  | 0.1 $^\circ\text{C}$ | 0 $\div$ +50 $^\circ\text{C}$   |
|                 | Relative humidity (RH)        | $\pm 3\%$ when RH $< 70\%$<br>$\pm (3\% + 1\% \text{ RH})$ when RH $\geq 70\%$           | 0.1%                 | 5 $\div$ 95%                    |
|                 |                               |  |                      | 5 $\div$ 95%                    |

modeling of green façades were made in the last years [47,50]. A few studies have developed dedicated heat transfer models through vegetated facades [36,37,51–53]: among these models, the one defined by Susorova offers an improvement in the modeling of transpiration, radiative and convective heat exchange between the plant layer, the façade, the surrounding environment and the ground. The main novelty is the use of individual plant features to simulate the impacts of vegetated walls on facades' thermal performance [47].

The present study takes advantage of these capabilities by modelling the VGS through the green facade energy balance discussed by Susorova [47] and then implemented into the Vertical Foliage Component (VFC) – called Type 9644 – in TRNSYS, [54,55]. The VFC model is based on a one-dimensional surface energy balance, applied to a control volume composed by a vertical vegetation layer coupled with the bare wall of the building. The energy balance includes the shortwave radiation from the sun (SR), the long-wave radiation exchanged with the ground (LR<sub>g</sub>) and the sky (LR<sub>s</sub>), the radiant exchange between the foliage and the bare wall surface (XR), the heat transferred by convection (C) and evapotranspiration (E) to the outdoor air. The energy balance on the green façade can thus be expressed by the following equation:

$$(SR + LR + XR + C + E) - Q = S \quad (1)$$

where (Q) is the heat flux transmitted by conduction from the outer surface through the inner layers of the wall, and (S) is the heat storage in the same wall. Fig. 3 summarizes the energy balance described above.

All the heat fluxes involving the vegetation layer of the green façade model are reported as follows:

$$SR = \tau \cdot I_s \cdot \alpha_w \quad (2)$$

$$LR = LR_s + LR_g = \tau \cdot \varepsilon_w \varepsilon_s \cdot \sigma \cdot F_s (T_s^4 - T_w^4) + \tau \cdot \varepsilon_w \varepsilon_g \cdot \sigma \cdot F_g (T_g^4 - T_w^4) \quad (3)$$

$$XR = (1 - \tau) \cdot \frac{\varepsilon_i \varepsilon_w}{\varepsilon_i + \varepsilon_w - \varepsilon_i \varepsilon_w} \cdot \sigma \cdot (T_i^4 - T_w^4) \quad (4)$$

$$E = \left[ \lambda \cdot g_v \cdot \frac{0.611 \cdot (RH - 1)}{p_a} \right] \cdot e^{\frac{17.5 \cdot (T_i - 273)}{T_i - 32}} \quad (5)$$

$$C = h \cdot (T_o - T_w) \quad (6)$$

The total radiation transmitted through a plant is expressed by the solar transmissivity coefficient ( $\tau$ ), which is calculated with the relationship developed by Monsi and Saeki [56]:

$$\tau = e^{-k \cdot LAI} \quad (7)$$

In Eq. (7), LAI is the Leaf Area Index of the plant and  $k$  is the radiation attenuation coefficient. The Leaf Area Index (LAI) is defined as the foliage area per unit soil surface beneath ( $\text{m}^2/\text{m}^2$ ), or as the one-sided leaf area per unit wall surface area in the case of VGSs. It is a key parameter for estimating the potential cooling effects of a vertical greenery layer, and depends on factors such as the plant physiology and the development phase of the canopy [57,58]. The radiation attenuation coefficient ( $k$ ) can vary between 0 and 1 and depends on the average leaves' orientation against the wall and the sun, as well as some plant geometric features [59,60].

The heat exchange by evapotranspiration process recurring in Eq. (5) is a function of the vapor conductance through the air ( $g_v$ ), which depends on the characteristic dimension and stomatal conductance of leaves. The plant stomatal conductance ( $g_s$ ) is defined as the rate of water vapor loss through the stomata of leaves during the transpiration phenomena, as determined by the degree of stomatal aperture [47,57]. Leaf stomatal conductance depends on the quantity of pores per leaf surface area and the pore size. Stomatal conductance tends to decrease with higher temperatures and lower relative humidity: typical stomatal conductance values for leaves vary in the range 0.2  $\div$  0.4  $\text{mol}/\text{m}^2\text{s}$  [47, 56,61]. The leaf typical dimension (D) has an important function in

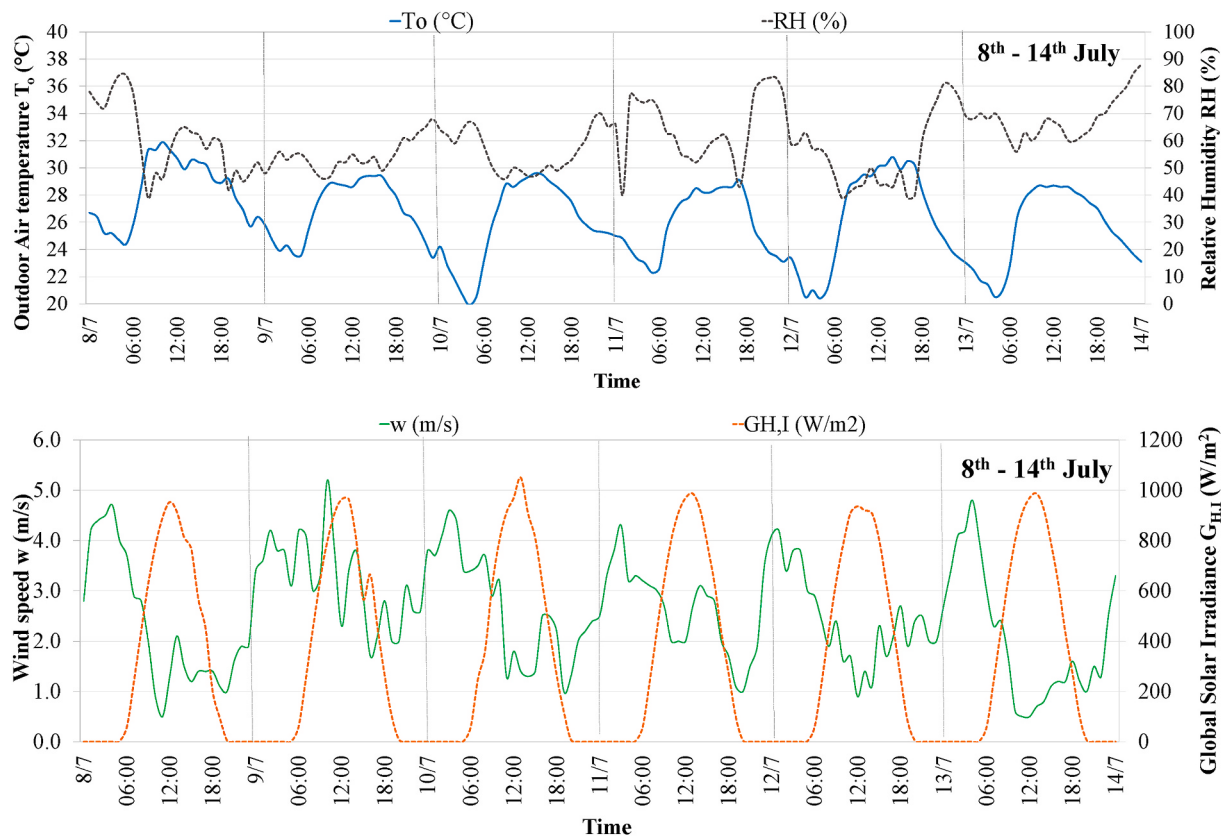


**Fig. 2.** Hourly values of outdoor air temperature and relative humidity (a), solar radiation and wind speed (b), recorded at the local weather station during the period 8-14 July 2022.

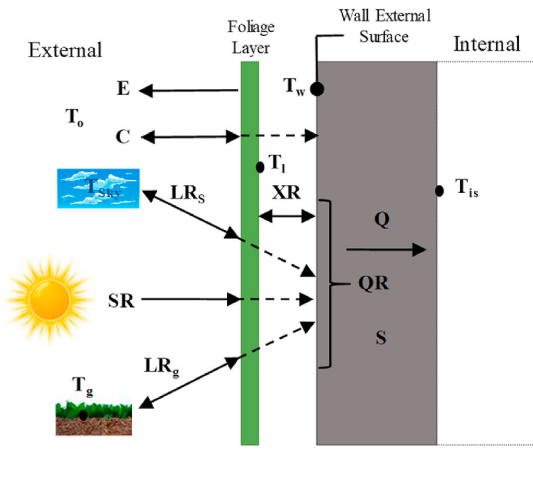


**Fig. 3.** Energy balance of a green façade as modelled with TRNSYS Type 9644 (adapted from Ref. [47]). (For interpretation of the references to color in this figure legend, the reader is referred to the Web version of this article.)

convective heat transfer and vapor conductance between the leaves and the air and, can be assumed equal to 70% of the average leaf width [57].

The leaf temperature ( $T_l$ ) recurring in Eq. (4) is determined through the Campbell's energy balance that includes the solar radiation absorbed by the leaf ( $SR_l$ ), long-wave thermal radiation exchanged between leaf and sky ( $L_{sl}$ ) and ground ( $L_{lg}$ ), the radiant heat exchange between leaf and bare wall ( $XR_l$ ), sensible heat loss ( $H_l$ ) and latent heat loss by transpiration ( $E$ ) through the leaf [56]. In this energy balance, the fraction of shortwave radiation which is not transmitted by the foliage

layer to the wall is partially absorbed by the leaf, as expressed by Eq. (8), where  $\alpha_l$  is the leaf absorptivity [57].

$$SR_l = I_l \cdot \alpha_l \quad (8)$$

The vegetation influences the convective heat transfer with the wall, since it decreases the wind speed at the vegetated wall surface. Considering this, the convective heat transfer coefficient ( $h$ ) of the wall in presence of the vertical vegetation layer is expressed as follows:

$$h = a + b \cdot (1 - 0.1 \cdot LAI) \cdot w + c \cdot (1 - 0.1 \cdot LAI) \cdot w^2 \quad (9)$$

where  $a$ ,  $b$ ,  $c$  are the material roughness coefficients, and  $w$  is the local wind speed [47,55].

The above described VFC model (Type 9644) is then coupled to the bare wall of the multizone building model component (Type 56), thus creating a complete TRNSYS simulation workflow. Fig. 4 shows the scheme of the coupling multizone building model to the green facade component in TRNSYS Simulation Studio.

The VFC model requires the following inputs:

- Weather data: air temperature, relative humidity, wind speed and direction, fictive sky temperature, solar irradiance on the vertical surface;
- Vegetated data: Leaf Area Index (LAI), solar absorptance of the leaves ( $\alpha_l$ ), thermal emissivity of the leaves ( $\epsilon_l$ ), plant stomatal conductance ( $g_s$ ), leaf characteristic dimension (D), and leaf radiation attenuation coefficient (k);
- Ground temperature ( $T_g$ );
- External surface temperature ( $T_w$ ) of bare wall behind the vegetation layer.  $T_w$  is calculated through the energy balance on the external surface of the external wall of the Multizone building model (Type 56), but without the inclusion of the greenery layer.

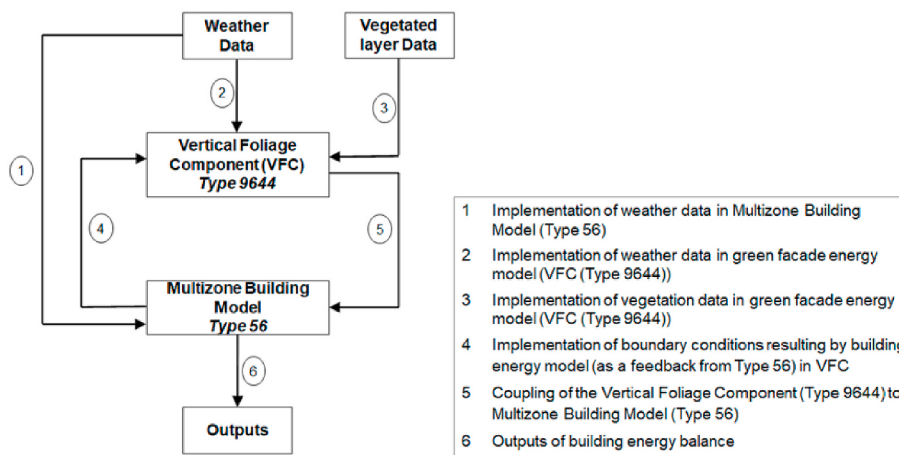


**Fig. 4.** Coupling VFC (Type 9644) to the Multizone Building Model (Type 56) in TRNSYS Simulation studio (adapted from Ref. [46]).

On the other hand, the output data from the VFC are:

- Total radiant heat flux (QR) acting on the external surface of the bare wall covered by foliage.
- Convective heat transfer coefficient (h) calculated for the external surface of the bare wall.

The total radiant heat flux computed by the VFC is then used by the wall model of Type 56 as an external surface gain, whereas the convective heat transfer coefficient computed by the VFC is applied to the bare wall of Type 56.

The main assumptions and limitations of the vegetation model in the VFC can be summarized as follows [47,55]:

- Leaves have the same distribution and orientation in the vegetation layer and, therefore, individual leaves' angles are not accounted for;
- All leaves have the same values of LAI and radiative properties;
- Wind speed is assumed to be constant for low-rise facades;
- Vegetation parameters such as leaf typical dimension (D), radiation attenuation coefficient (k), and plant stomatal conductance ( $g_s$ ) cannot be varied with the season.

Finally, different statistical indices such as the Mean Absolute Error (MAE), the Root Mean Square Error (RMSE), the index of agreement (d), the Pearson's coefficient (r), and the coefficient of determination ( $R^2$ ) were used to quantify the discrepancies between experimental and simulated data according to Ref. [17].

#### 4. Case study

##### 4.1. Building's site and thermal features

The experimental site is located in Catania, a city along the Mediterranean coast in Southern Italy (latitude 37°30' North, Longitude 15°04' East) characterized by a warm and temperate climate defined as Csa according to the international Köppen-Geiger climate classification [62].

The experimental set-up consists of two prefabricated modules located at the local University Campus in an area free from obstacles (both buildings and trees) so that the modules are not shaded. The two mock-ups have the same shape, materials and construction assemblies, and the only difference is a vertical greenery system installed on one of them on the west-oriented wall. The modules are made with lightweight and self-supporting structure (2.50 x 2.50 x 3.00 m<sup>2</sup> size) and are oriented to face the four main compass directions. Internally, the prefabricated modules consist of a single room without any air conditioning

system. Fig. 5 shows the installation area of the two investigated experimental mock-ups.

The opaque closures of the prefabricated modules are made with sandwich panels including an insulating polystyrene layer and two Oriented Strand Board (OSB) finishing layers. The floor and the roof have the same composition as the walls. Further details are available in Table 3. A horizontal unventilated air gap of about 5 cm is included between the walkable floor and the base structure of the module. The internal floor surface is finished in laminate with parquet effects, while the roof is coated with a metallic corrugated sheet. On the other hand, the external door is made of white honeycomb steel, while the south-facing window is a PVC double-glazed fixture with an air gap of 15 mm. The external surfaces of the building roof and walls are finished with a white color. Fig. 6 shows the three-dimensional view of the two prefabricated modules.

The various layers of the building elements, and their thermal properties, are provided by the building company that realized the prefabricated modules. U-values of the opaque vertical and horizontal closures were obtained through heat flow meter tests carried out by "Domus Corporation" according to ISO 9869 method [63].

##### 4.2. The green façade and the modelling assumptions

The proposed vertical greenery system is an indirect green façade constituted by a support structure to sustain a creeping plant species. A single type of evergreen climbing plant, namely "*Trachelospermum Jasminoides*", was installed on the west-facing wall of one of the two prefabricated modules. The west orientation was selected because, at this latitude, it is the most prone to overheating issues. Previous studies also indicated that the use of the Vertical Green Façade on west walls leads to maximum cooling effects in summer, if compared to other orientations [46].

The *Trachelospermum Jasminoides* is a climbing shrub with voluble stems belonging to the family of the *Apocynaceae*, commonly known as *false jasmine* or *rhincosperma*. It is an endemic species characterized by deep green, quite smooth and a sharp pointed leaf [35]. *Jasminoides* is a fast-growing plant that can climb up a trellis with ease until 6 m, with low cost of maintenance, it can withstand very high temperatures typical of torrid heat and it can tolerate sunny exposure characterized by intense solar radiation [35,64]. For these reasons, and because it requires moderate water and low quantity of fertilizer, it has been selected for this investigation.

The supporting structure of the climbing plant is a wood frame constituted by a grid dimension of 0.20 m x 0.50 m, placed at 10 cm from the prefabricated module. The framework is anchored to the lower part of a pot and to the top of the wall of the prefabricated module.



**Fig. 5.** Experimental mock-ups. a) 2D view of urban area; b) 2D view of the experimental area; c) 3D view of the prefabricated modules from north-west; d) 3D view of the prefabricated modules from east.

**Table 3**  
Assemblies and their thermo-physical parameters.

| Building Elements | Layer (From outer to inner side) | Thickness s (mm) | Thermal conductivity $\lambda$ (W/mK) | Specific heat $C_p$ (J/kgK) | Density $\rho$ (kg/m <sup>3</sup> ) | U-value (W/m <sup>2</sup> K) |
|-------------------|----------------------------------|------------------|---------------------------------------|-----------------------------|-------------------------------------|------------------------------|
| Wall/Roof         | Osb                              | 9                | 0.10                                  | 650                         | 600                                 | 0.50                         |
|                   | Polystyrene                      | 65               | 0.033                                 | 1450                        | 15                                  |                              |
|                   | Osb                              | 6                | 0.1                                   | 650                         | 600                                 |                              |
| Floor             | Air gap                          | 200              | 0.14                                  | 1008                        | 1.3                                 | 0.36                         |
|                   | Osb                              | 6                | 0.1                                   | 650                         | 600                                 |                              |
|                   | Polystyrene                      | 65               | 0.033                                 | 1450                        | 15                                  |                              |
|                   | Osb                              | 6                | 0.1                                   | 650                         | 600                                 |                              |
| Window            | Glass                            | 4                | 1.00                                  | 750                         | 2500                                | 2.82                         |
|                   | Air gap                          | 15               | 0.025                                 | 1006                        | 1.20                                |                              |
|                   | Glass                            | 4                | 1.00                                  | 750                         | 2500                                |                              |



**Fig. 6.** Prefabricated modules: a-b) Module without VGS (P.M. 1); c-d) Module with VGS (P.M. 2).

Currently, the wall houses six plants rooted at the ground in wood pots of approximate dimensions of 1.29 m × 0.44 m and a height of 0.40 m. The soil in the pots is a porous soil composed by a mixture of peat, pumice, mineral aggregates, and other soil granules. The *Jasminoides* species has LAI values varying through the year in the range of 2.0–4.0 m<sup>2</sup>/m<sup>2</sup> [35]. The leaves can be characterized by the following typical values of their optical and thermal properties [64,65]: 0.54 for solar absorptivity, 0.32 for reflectivity, 0.14 for transmissivity and 0.96 for IR emissivity.

All data inputs of the VFC (Type 9644) used in the TRNSYS simulation scheme are summarized in Table 4. Fig. 7 shows the picture of the west oriented green façade, taken during the experimental measurement period (8th to 14<sup>th</sup> July 2022).

As it can be observed from Table 4, some of the input parameters required by the VFC are calculated by TRNSYS, namely the total tilted surface irradiation  $G_t$ , the effective sky temperature  $T_s$  and the ground temperature  $T_g$ . The total tilted surface irradiation is an output of the weather type of TRNSYS and is calculated by first obtaining beam and diffuse radiation on a horizontal surface from total radiation based on the relationships developed by Reindl [66], and transposed to the tilted

**Table 4**

Inputs of the Vertical Foliage Component (VFC) for the *Trachelospermum Jasminoides* species.

| No | Name            | Description                             | Unit                            | Value                      |
|----|-----------------|---|---------------------------------|----------------------------|
| 1  | LAI             | Leaf Area Index                         | $\text{m}^2/\text{m}^2$         | 2.0 [35]                   |
| 2  | $\alpha_l$      | Leaf absorptance                        | -                               | 0.54 [64,65]               |
| 3  | $G_t$           | Total tilted surface irradiation        | $\text{kJ}/\text{m}^2/\text{h}$ | Calculated [66]            |
| 4  | w               | Wind speed                              | $\text{m}/\text{s}$             | From local weather station |
| 5  | RH              | Relative Humidity                       | %                               | From local weather station |
| 6  | $p_a$           | Atmospheric pressure                    | atm                             | From local weather station |
| 7  | $T_o$           | Dry-bulb temperature                    | $^\circ\text{C}$                | From local weather station |
| 8  | $T_s$           | Effective sky temperature               | $^\circ\text{C}$                | Calculated [67,68]         |
| 9  | $T_g$           | Ground Temperature                      | $^\circ\text{C}$                | Calculated [69]            |
| 10 | $T_{so}$        | Outside surface temperature of the wall | $^\circ\text{C}$                | TRNBuild output            |
| 11 | $S_w$           | Wall Area                               | $\text{m}^2$                    | 5.65                       |
| 12 | $\alpha_w$      | Wall absorptance                        | -                               | 0.30                       |
| 13 | a               | Coefficient for convection on bare wall | $\text{W}/\text{m}^2\text{K}$   | 12 [47,55]                 |
| 14 | b               | Coefficient for convection on bare wall | $\text{J}/\text{m}^3\text{K}$   | 6 [47,55]                  |
| 15 | c               | Coefficient for convention on bare wall | $\text{Js}/\text{m}^4\text{K}$  | 0 [47,55]                  |
| 16 | $g_s$           | Leaf Stomatal Conductance               | $\text{mol}/\text{m}^2\text{s}$ | 0.40 [14,15,25]            |
| 18 | D               | Leaf typical dimension                  | m                               | 0.11 [14,15,25]            |
| 19 | k               | Leaf radiation attenuation coefficient  | -                               | 0.7 [64,70,71]             |
| 20 | $\varepsilon_l$ | Leaf emissivity                         | -                               | 0.96 [64,65]               |
| 21 | $\varepsilon_w$ | Wall emissivity                         | -                               | 0.90                       |
| 22 | $\varepsilon_g$ | Ground emissivity                       | -                               | 0.90                       |
| 23 | $\varepsilon_s$ | Sky emissivity                          | -                               | 0.90                       |
| 24 | $F_g$           | Ground view factor                      | -                               | 0.5                        |
| 25 | $F_s$           | Sky view factor                         | -                               | 0.5                        |



**Fig. 7.** West-oriented wall of the prefabricated module with VGS. a) Growing state during the experimental measurements campaign; b) Evergreen climbing plant; c) Framework of the support structure; d) plan view of the prefabricated module.

surface through the Hay and Davies' model [66]. The effective sky temperature ( $T_s$ ) is instead calculated as a function of the ambient temperature, air humidity, cloudiness factor of the sky, and the local air pressure, according to the algorithm described in mathematical reference of TRNSYS software [67,68], while the ground temperature ( $T_g$ ) is calculated according to the Kasuda's relationship [69].

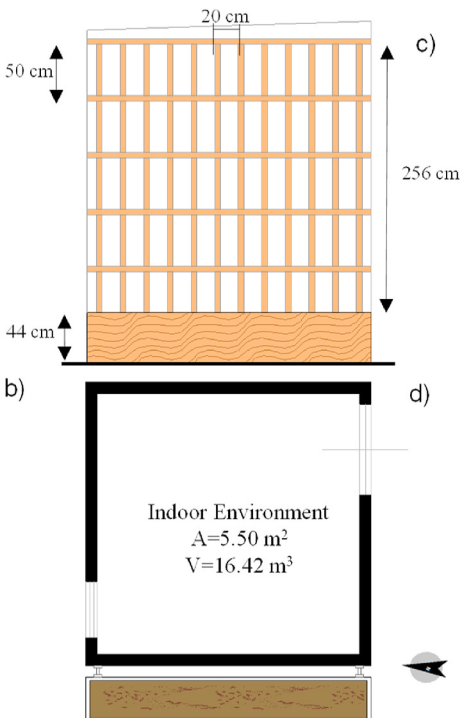
The Leaf Area Index (LAI) value was assumed according to data obtained by LAI measurements carried out on *Jasminoides* species by Convertino [65]. The radiative properties of leaves such as Leaf absorptance ( $\alpha_l$ ) and emissivity ( $\varepsilon_l$ ) were determined by means of measurements conducted on the same *Jasminoides* species as reported in previous studies [35,64,65]. The radiation attenuation coefficient was calculated by means of the equation described in Ref. [70] based on a suggested average leaf inclination angle of about 40° [64,71]. The stomatal conductance and leaf typical dimensions' values were instead adopted from the literature on biophysics [14,15,25].

The experimental system was equipped with a drip irrigation system that is switched on every day of the week from 07:00 to 07:10, with a water flow rate of 20 mm per hour.

The area of the wall behind the foliage ( $S_w$ ) is set to 5.65  $\text{m}^2$  in order to consider the presence of the pots and that the vegetation layer does not fully cover the wall. The values of solar absorptance ( $\alpha_w$ ) and thermal emissivity ( $\varepsilon_w$ ) of the bare walls of the two experimental mock-ups were provided by the building company that realized the prefabricated modules. It was assumed that the external surface of the bare wall is made of a material with a medium-rough surface for which the material coefficients for the calculation of the convective coefficient are 12, 6, and 0 [47,55]. The simulations of the TRNSYS model are performed in free running conditions with a time step of 1 h.

#### 4.3. Validation of the thermal model

The predicted trends of indoor air temperature and internal surface temperature for both configurations (bare façade and green façade) are compared to the recordings of the experimental campaign during the



summer week (8th to 14th July). The comparison is shown in Fig. 8 and reveals a very good agreement between measurements (solid grey lines) and simulations (dashed grey lines) for both configurations throughout the analyzed period. Indeed, the simulated trends are almost identical to those measured during daytime, while at nighttime and sunrise the simulations tend to slightly underpredict the indoor air temperature, probably because of an overestimation of the infrared radiant exchange with the sky. However, such discrepancy never exceeds 1 °C.

Furthermore, Fig. 9 compares the measured and the simulated surface temperatures on the internal side of the west oriented wall, during the same measurement period. The comparison reveals that simulated and measured profiles show high similarity also for the internal surface temperature, with slight differences corresponding to the periods previously reported for indoor air temperature.

Overall, the comparison between experimental and simulated data indicates a good agreement. With the aim of further substantiating the validation exercise, the statistical indices listed in Section 3.2 are calculated and reported in Table 5. In the prefabricated module without the green facade, the percentage of error is below 2% and the MAE amounts to 0.23 °C. The excellent correlation is confirmed also by the high values for both the correlation coefficient ( $r$ ) and the coefficient of determination ( $R^2$ ), which exceed 0.96.

Regarding the green facade configuration, the statistical indices confirm the excellent agreement between predicted and measured data (MAE = 0.21 °C and RMSE = 0.35 °C). The Pearson's correlation coefficient is  $r = 0.99$ , while the index of agreement ( $d$ ) approaches 0.97 during the investigated period. Similar results are also reported for the internal surface temperature. A graphical representation of the results obtained by the simulations is given also in Figs. 10 and 11, where regression lines are plotted for both indoor air temperature and internal surface temperature of the wall with and without the vegetation.

## 5. Results and discussion

### 5.1. Investigated green façade configurations

With the aim of evaluating in a more comprehensive way the cooling effect achievable by a green façade, a comparison between the “*Trachelospermum Jasminoides*” and another plant species commonly adopted in the Mediterranean area, namely the “*Hedera Helix*”, is presented hereafter. Indeed, *Hedera Helix* is an evergreen climbing plant species able to adapt to cold periods while also being photosynthetically productive during daytime [72]. The leaves are characterized by  $\varepsilon_l = 0.95$  and  $\alpha_l = 0.78$  according to typical spectral properties [73], while the Leaf Area Index (LAI) varies from a minimum of 2.7 to a maximum of  $4.3 \text{ m}^2 \text{ m}^{-2}$ , the leaf typical dimension ( $D$ ) can be assumed equal to 0.05 m, the radiation attenuation coefficient ( $k$ ) is equal to 0.7 and the stomatal conductance ( $g_s$ ) amounts to  $0.2 \text{ mol m}^{-2} \text{ s}^{-1}$  [74–76].

Because of the intrinsic variability of the LAI according to seasonal temperature, plant age, nutrients availability, growing process and other factors [77], various LAI values are considered in the comparison between green facades scenarios with *Trachelospermum Jasminoides* and *Hedera Helix*. In particular, four different scenarios of the green façade have been examined, by varying not only the plant species (*Trachelospermum Jasminoides*, T.j., and *Hedera Helix*, H.h.), but also the LAI value from a minimum to a maximum value representative of both the initial state (GF1, T.j. LAI = 2 and GF3, H.h. LAI = 2.7) and the maximum development state of the plants (GF2, T.j. LAI = 4 and GF4, H. h. LAI = 4.3). The base scenario (BS), instead, represents the bare wall configuration without any vertical greenery layer.

The performance of the different green facade configurations has been compared by looking at the internal surface temperature, the external surface temperature, and the heat flux during the analyzed summer week.

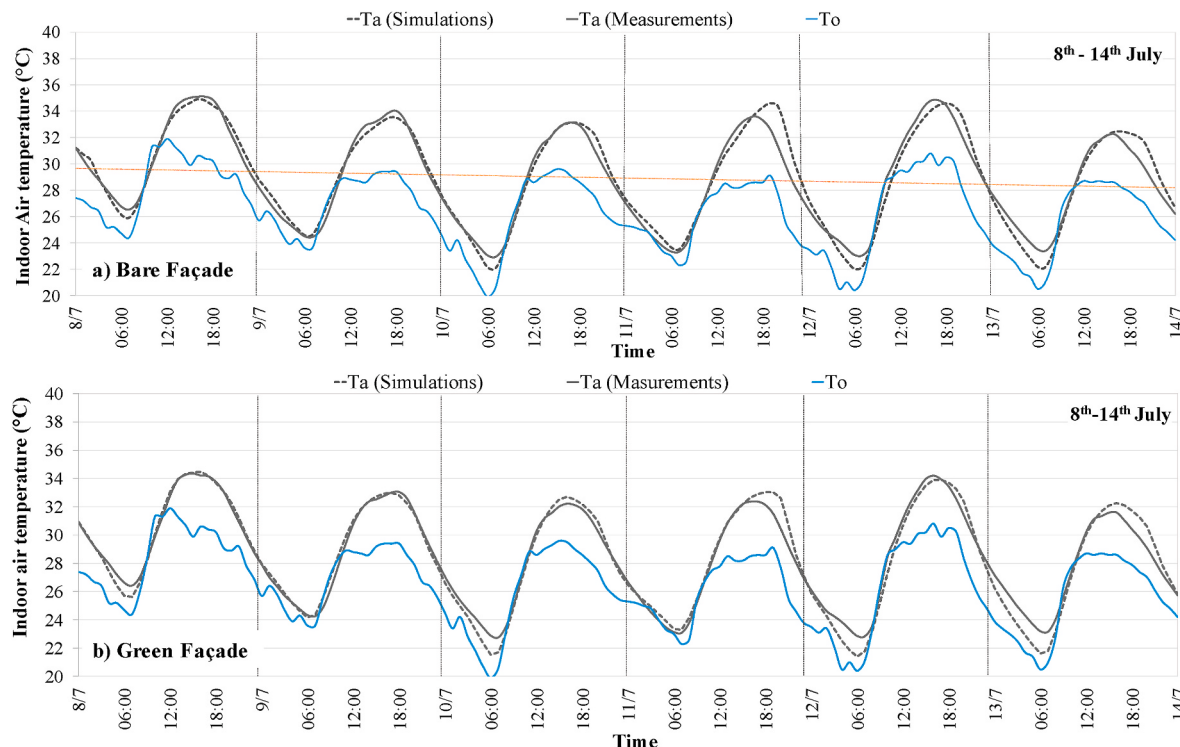


**Fig. 8.** Comparison between simulated and measured indoor air temperature during the period 8–14 July 2022. a) Bare Façade; b) Green Façade. (For interpretation of the references to color in this figure legend, the reader is referred to the Web version of this article.)

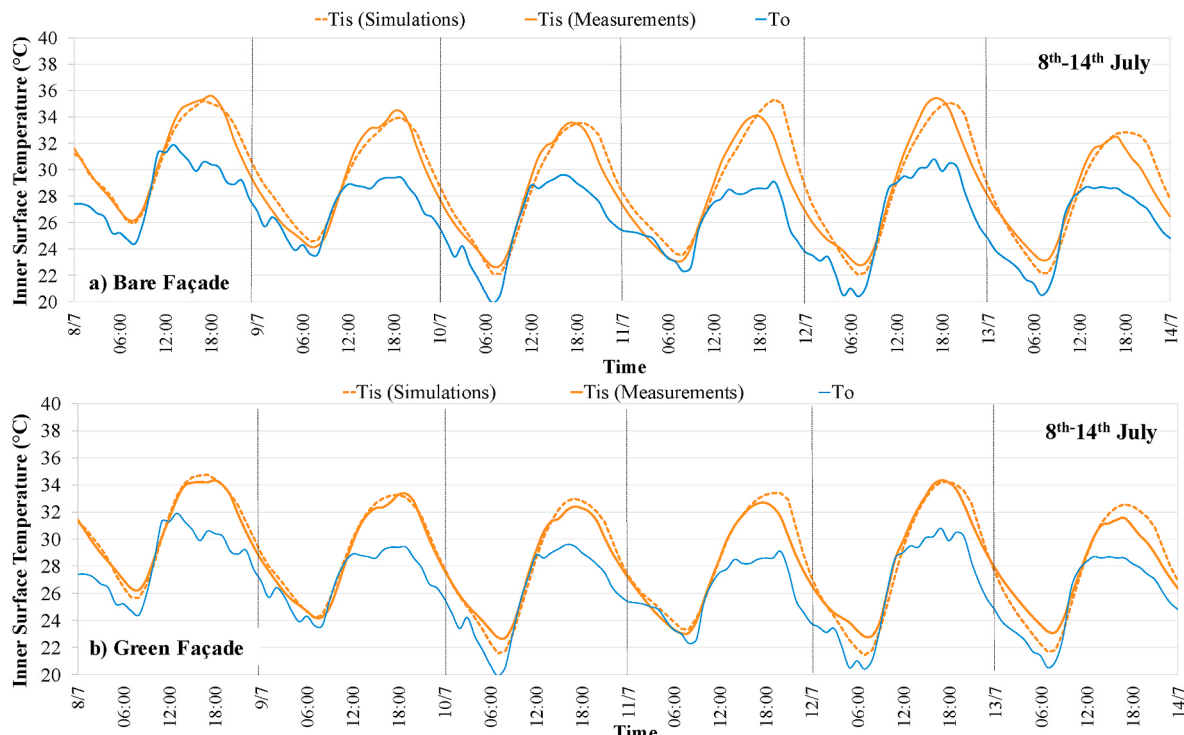


**Fig. 9.** Comparison between simulated and measured indoor surface temperature of the west oriented wall during the period 8–14 July 2022. a) Bare Façade; b) Green Façade. (For interpretation of the references to color in this figure legend, the reader is referred to the Web version of this article.)

**Table 5**

Validation indices of the TRNSYS model for bare façade and green façade configurations.

| Variable        | Statistical indices and units | Wall configurations |              |
|-----------------|-------------------------------|---------------------|--------------|
|                 |                               | Bare Façade         | Green Façade |
|                 |                               | (Module 1)          | (Module 2)   |
| T <sub>a</sub>  | % error                       | -                   | 2.1          |
|                 | MAE                           | °C                  | 0.57         |
|                 | RMSE                          | °C                  | 0.76         |
|                 | d                             | -                   | 0.98         |
|                 | r                             | -                   | 0.98         |
|                 | R <sup>2</sup>                | -                   | 0.96         |
| T <sub>is</sub> | % error                       | -                   | 1.06         |
|                 | MAE                           | °C                  | 0.31         |
|                 | RMSE                          | °C                  | 0.53         |
|                 | d                             | -                   | 0.99         |
|                 | r                             | -                   | 0.97         |
|                 | R <sup>2</sup>                | -                   | 0.96         |

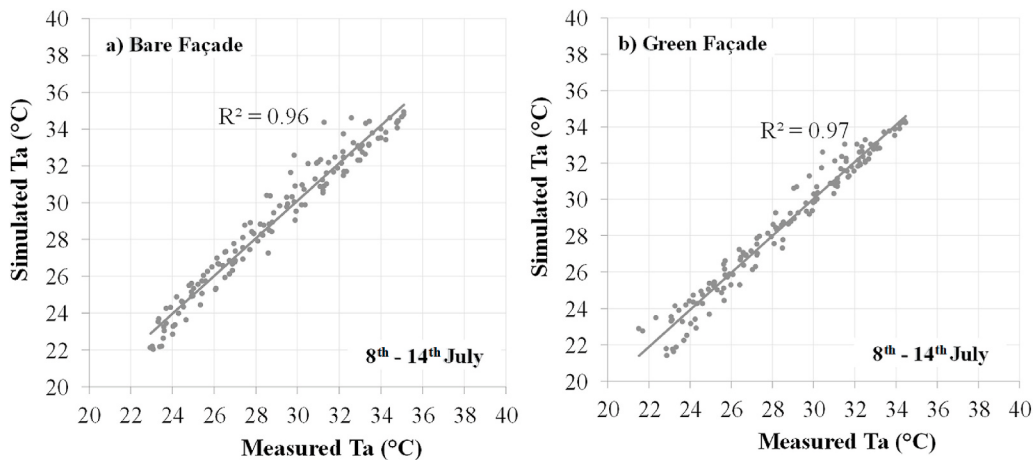
## 5.2. Surface temperature and heat flux analysis

Fig. 12 shows that, in the base scenario (BS), the internal surface temperature varies from a minimum value of 21.3 °C to a maximum value of 34.8 °C, achieved at around 5.00 p.m.

Table 6 reports the maximum reduction of T<sub>is</sub> achieved by means of the proposed green facade configurations, in comparison with the base scenario (BS). The green façade with *Trachelospermum Jasminoides* plant species and LAI of 2.0 m<sup>2</sup>/m<sup>2</sup> (GF1 configuration) reduces the peak values of T<sub>is</sub> up to 1.1 °C in the hottest hours. Under full flourishing conditions of the plants, green façade (GF2 configuration) allows reducing the T<sub>is</sub> by a maximum value of 1.6 °C during daytime. In the

case of *Hedera Helix* plant species, a reduction of T<sub>is</sub> by a maximum of 1.3 °C can be obtained for LAI values of 2.7 m<sup>2</sup>/m<sup>2</sup> (GF3 configuration), and a decrease by 1.6 °C under full development conditions of the foliage layer (GF4) respectively in the warmest hours of the sunny days. During the night and in the morning, the trend of T<sub>is</sub> is almost the same for all investigated wall configurations. However, it can be observed that a vertical greenery layer with low LAI values, i.e. corresponding to the initial state of the growing process (LAI = 2.0 m<sup>2</sup>/m<sup>2</sup> for *Trachelospermum Jasminoides* and LAI = 2.7 m<sup>2</sup>/m<sup>2</sup> for *Hedera Helix*), is already effective. A denser foliage layer (GF2 and GF4 configurations) provides only limited further reductions in the peak surface temperature value (Fig. 12). It is worth highlighting that only few previous numerical studies rely on dynamic simulations to investigate the reduction in the internal surface temperature. Although the back wall structure for the green façade is different from this experimental setup (see Section 2), and there are also different climate and boundary conditions, the outcome of this study is comparable to the numerical and experimental studies [12,40] reported in Table 1. In order to evaluate the effects on the local microclimate, the external surface temperature (T<sub>os</sub>) was calculated as well for each facade scenario, since this parameter can be used as an indicator of the contribution to the Urban Heat Island (UHI) phenomenon. Fig. 13 thus shows the simulated daily profiles of external surface temperature of the west-facing wall in the base case (BS) and in the proposed green facade configurations (GFs). For the base case (BS), the external surface temperature varies from a minimum value of 18.6 °C to a peak value of 37.8 °C, achieved around 5.00 p.m.

Table 6 also suggests that the addition of a vertical greenery layer consisting of *Jasminoides* climbing plant species with LAI = 2.0 m<sup>2</sup>/m<sup>2</sup> allows a reduction in the peak external surface temperature exceeding 7.0 °C in the afternoon hours of a sunny day, mainly due to the shading effect of the plants. Under full development conditions of the foliage



**Fig. 10.** Linear regression for indoor air temperature (measured vs simulated). a) Bare façade; b) Green façade.

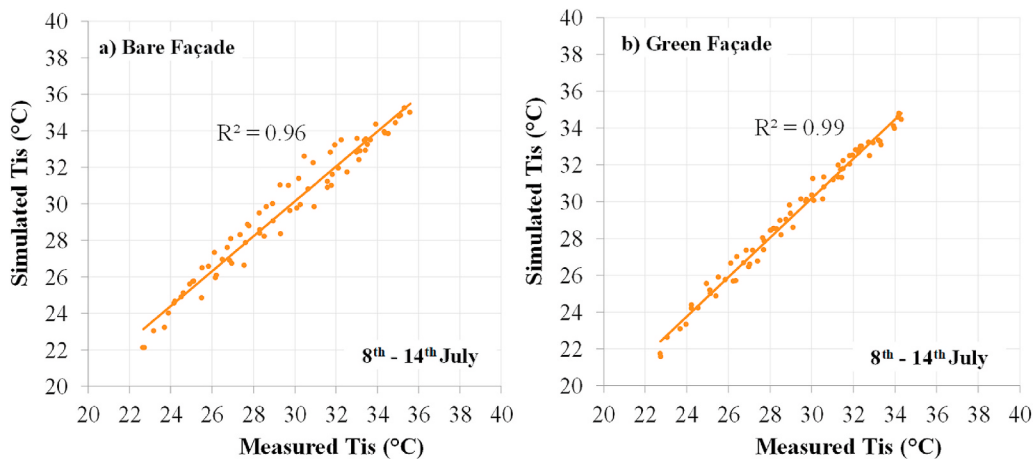


**Fig. 11.** Linear regression for indoor surface temperature (measured vs simulated). a) Bare façade and b) Green façade. (For interpretation of the references to color in this figure legend, the reader is referred to the Web version of this article.)

layer ( $LAI = 4.0 \text{ m}^2/\text{m}^2$ ), the green façade (GF2 configuration) can reduce the peak of  $T_{os}$  by a maximum of  $9.5^\circ\text{C}$ . There are no numerical studies on indirect green façades with *Jasminoides* against which comparing the reduction in the peak external surface temperature achieved in the present study, which is however comparable to the

experimental results reported by Vox [35]. In the case of *Hedera Helix*, the green façade shows a reduction in the peak values of  $T_{os}$  as high as  $8.6^\circ\text{C}$  for  $LAI = 2.7$  (GF3 scenario), and  $10.5^\circ\text{C}$  in the case of full development of the vegetation layer (GF4 scenario). Despite the difference in the back wall structure, the orientation of the wall and the

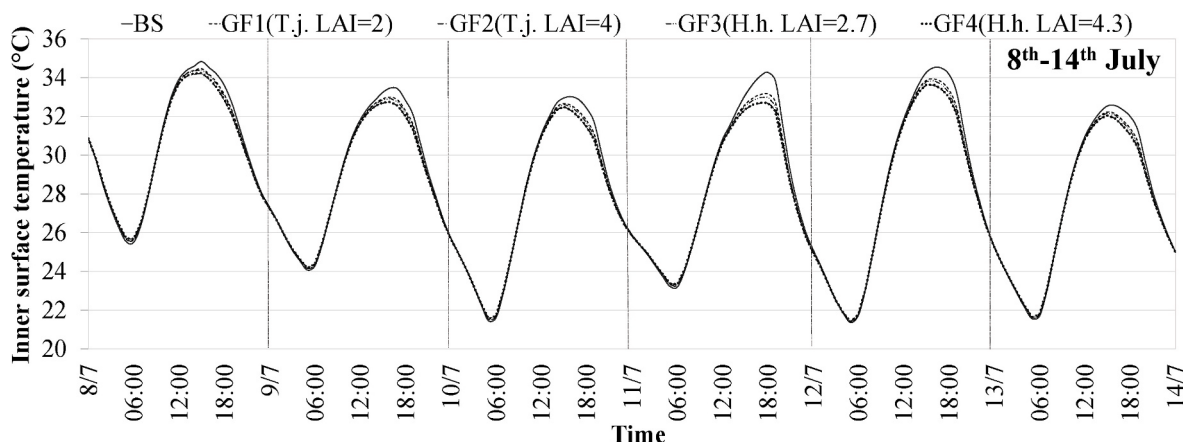


**Fig. 12.** Simulated daily profiles of internal surface temperature (Tis) of the west-oriented wall in the base case and the investigated green facades configurations during 8th-14th July.

**Table 6**

Peak surface temperature and heat flux reductions for the investigated green facade scenarios (GFs) with respect to the bare wall.

| Parameter                | Unit | GF1 (T.j.<br>LAI = 2.0) | GF2 (T.j.<br>LAI = 4.0) | GF3 (H.h.<br>LAI = 2.7) | GF4 (H.h.<br>LAI = 4.3) |
|--------------------------|------|-------------------------|-------------------------|-------------------------|-------------------------|
| $(\Delta T_{is})_{max}$  | °C   | 1.1                     | 1.6                     | 1.3                     | 1.6                     |
| $(\Delta T_{os})_{max}$  | °C   | 7.4                     | 9.5                     | 8.6                     | 10.5                    |
| Peak heat flux           | W    | 323                     | 79                      | 171                     | 33                      |
| Peak heat flux reduction | %    | 77                      | 96                      | 89                      | 97                      |

different modelling of vertical greenery, under full development of the foliage layer the results are close to the findings of previous numerical studies [22,40]. Although the climate conditions are different, indirect green façade with *Hedera Helix* plant species allows reductions in the peak external surface temperature like those achieved in experimental studies [43,45].

It is possible to observe that, looking at vertical vegetation layer with lower LAI values (GF1 and GF3), *Hedera Helix* plants showed better results than *Trachelospermum Jasminoides* both on internal and external surface temperature of the walls, despite the leaves of *Hedera helix* have higher solar absorptivity values than *Jasminoides*. This result is most probably related to the different LAI values.

Fig. 14 shows the simulated daily profiles of the heat flux transferred

on the external surface of the west facing wall, in all simulated cases.

The plots show an incoming heat flux almost all day long, from 9:00 to 19:00, while heat is released at night and in the early hours of the morning. The maximum heat flux occurs at around 17:00 for all investigated configurations, meaning that it is in phase with the typical solar radiation profile on a west-facing wall. The time trend for the bare wall (Bs) shows peak values exceeding 1 kW, whereas the heat released at night is typically smaller than 200 W. Table 6 reports the peak values and the corresponding reduction achieved by means of the green facades in comparison with the base scenario (BS), whose peak value is 1394 W.

The analysis trends depicted in Fig. 14 highlight that the green façade with LAI = 2.0 m<sup>2</sup>/m<sup>2</sup> (GF1) allows to remarkably reduce the peak value of the incoming heat flux in the prefabricated module (by 77%).

It is worth observing that the green façade configurations with denser vegetation layer (GF2, GF4) increase the heat losses towards the outdoor environment, and generate a quite flat profile for the heat flux. Finally, although the thermophysical and radiative properties of the plants are different, GF2 and GF4 configurations show very similar trends during the analyzed period: this suggests that high LAI values imply similar performance for the different species, and confirms that LAI is the parameter that most influences the thermal performance of green facades.

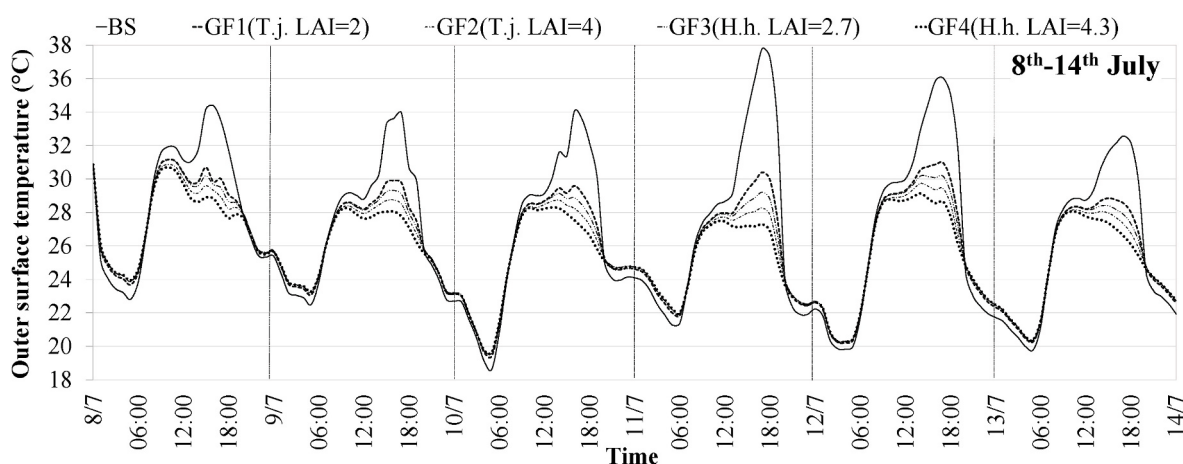


Fig. 13. Simulated daily profiles of external surface temperature (Tos) of the west-oriented wall in the Base case (BS) and investigated green facades configurations (GFs) during period 8th-14th July.

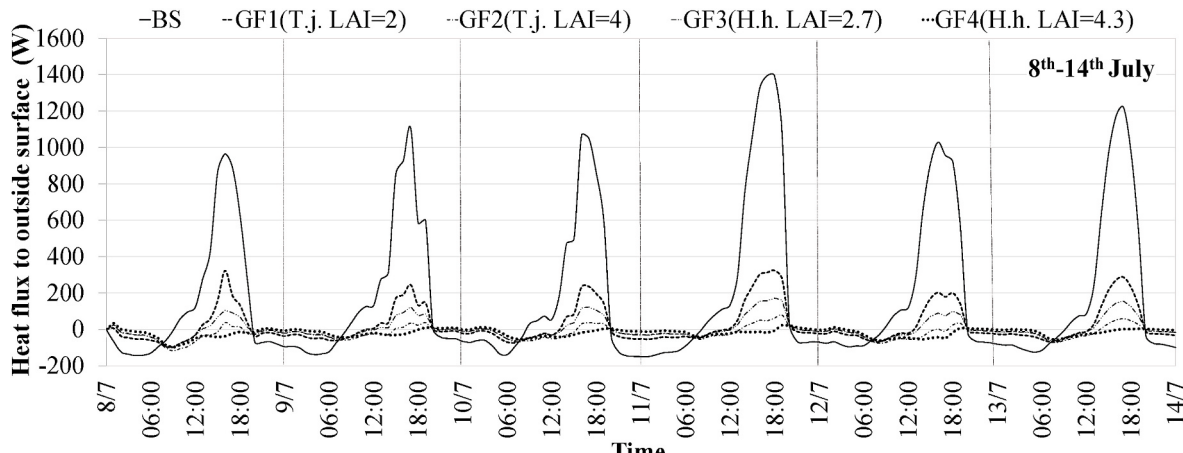


Fig. 14. Simulated daily profile of the heat flux through the west-facing wall in the Base scenario (BS) and green façade configurations (GFs) during the analyzed period (8th-14th July).

## 6. Conclusions

The present paper investigated the effectiveness of a green façade in improving summer indoor thermal conditions of a lightweight and well-insulated prefabricated test room by means of both experimental measurements and dynamic thermal simulations in TRNSYS through a novel dedicated Type coupled with the multizone building Type. To this aim, two identical full-scale experimental mock-ups were installed and monitored at the University Campus of Catania (Italy), which differ only in the west façade composition (one of them is equipped with *Trachelospermum Jasminoides* evergreen climbing plant, while the other one is not). The monitoring campaign, conducted during a typical summer week (from 8th to 14th July in 2022), allowed to validate the TRNSYS model.

The results of the experimental campaign revealed that the green façade can reduce the indoor air temperature and internal surface temperature up to 1.0 °C and 1.1 °C, respectively, in the hottest hours. The validation exercise also reveals an excellent correlation ( $R^2 = 0.97$  for indoor air temperature,  $R^2 = 0.99$  for internal surface temperature) between experimental measurements and numerical simulations: this confirms the goodness of the novel Type in TRNSYS, which was then used to understand the role of different climbing plant species and the Leaf Area Index on the thermal performance of the test room.

To this aim, four different scenarios of the green façade have been compared with the base case, by varying the plant species (*Trachelospermum Jasminoides* and *Hedera Helix*) for two values of LAI assumed as representative of the growing process of the plants. The green façade with *Trachelospermum Jasminoides* and LAI = 2.0 m<sup>2</sup>/m<sup>2</sup> allows to reduce the maximum value of internal surface temperature by 1.1 °C, and the external surface temperature by 7.4 °C, on the wall west facing. Moreover, the peak of the incoming heat flux is reduced by 78%. The results also show that a green façade with *Hedera helix* allows even better performance when the foliage layer is at initial and intermediate state of the growing process. Under full foliage development conditions of the selected plants, the performance of the green facades is almost the same with both species, which suggests that the LAI is the parameter with the highest influence on the thermal performance. Under these conditions, the incoming heat flux can be strongly attenuated (by around 96%), showing also a quite flat daily profile, the internal surface temperature is reduced by 1.6 °C and the external surface temperature can be reduced of 10.5 °C. The latter result is very important because it can also help in the UHI mitigation in mild Mediterranean areas.

Based on these findings, future developments of the research are planned to assess the role of the wall assembly behind the vegetation layer on the performances achievable by a green façade in terms of thermal mass and insulating layer's presence and position.

## CRediT authorship contribution statement

**Maurizio Detommaso:** Writing – original draft, Visualization, Software, Formal analysis. **Vincenzo Costanzo:** Writing – review & editing, Writing – original draft, Methodology, Investigation, Conceptualization. **Francesco Nocera:** Writing – review & editing, Supervision, Investigation, Conceptualization. **Gianpiero Evola:** Writing – review & editing, Visualization, Investigation.

## Declaration of competing interest

The authors declare that they have no known competing financial interests or personal relationships that could have appeared to influence the work reported in this paper.

## Data availability

Data will be made available on request.

## Acknowledgements

The authors acknowledge that the experimental mock-ups are made available in the framework of the ongoing research project “BETA Intradepartmental Project: Thermo-hygrometric well-being in internal and external environment and energy saving through vertical greenery systems (VGS)” taking place at the University of Catania. The authors would also like to thank the “Laboratorio di Sostenibilità Energetica ed il controllo ambientale (SECA)”, University of Catania, for providing the measuring instruments, and Krzysztof Grabowiecki and Bartosz Katski who developed the TRNSYS component VFC Type 9644 used in this study.

## Nomenclature

|                 |  |
|-----------------|--|
| $I_t$           | total irradiance on the wall surface (W•m <sup>-2</sup> )  |
| $\alpha_l$      | solar absorptance of the leaves (-)  |
| $\alpha_w$      | solar absorptance of the bare façade (-)   |
| $\tau$          | transmissivity of the foliage layer (-)  |
| $\varepsilon_w$ | emissivity of the bare façade (-)  |
| $\varepsilon_s$ | sky emissivity (-)   |
| $\varepsilon_l$ | leaf emissivity (-)  |
| $\varepsilon_g$ | ground emissivity (-)  |
| $\sigma$        | Stefan-Boltzmann constant (W•m <sup>-2</sup> •K <sup>-4</sup> )                                    |
| $F_s$           | view factor between the wall and the sky (-)   |
| $F_g$           | view factor between the wall and the ground (-)  |
| $T_g$           | ground surface temperature (K)   |
| $T_l$           | leaf temperature (K)   |
| $T_o$           | outdoor air temperature (K)  |
| $T_s$           | sky temperature (K)  |
| $T_w$           | façade surface temperature behind the vegetation (K)   |
| $h$             | convective heat transfer coefficient of the vegetated façade (W•m <sup>-2</sup> •K <sup>-1</sup> ) |
| $\lambda$       | latent heat of vaporization (kJ•kg <sup>-1</sup> )   |
| $g_v$           | current effective vapor conductance (mol•m <sup>-2</sup> •s <sup>-1</sup> )                        |
| $RH$            | relative humidity (%)  |
| $p_a$           | atmospheric pressure at the sea level (kPa)  |
| $v$             | wind speed (m/s)   |

## References

- [1] S. Chapman, J.E.M. Watson, A. Salazar, M. Thatcher, C.A. Mc Alpine, The impact of urbanization and climate change on urban temperatures: a systematic review, Landsc. Ecol. 32 (10) (2017) 1921–1935, <https://doi.org/10.1007/s10980-017-0561-4>.
- [2] M. Antrop, Landscape change and the urbanization process in Europe, Landsc. Urban Plann. 67 (2004) 9–26, [https://doi.org/10.1016/S0169-2046\(03\)00026-4](https://doi.org/10.1016/S0169-2046(03)00026-4).
- [3] Y.H. Chen, J.T. Wu, K. Yu, Evaluating the impact of the building density and height on the block surface temperature, Build. Environ. 168 (1) (2020), 106493.
- [4] H. Akbari, C. Cartalis, D. Kolokotsa, A. Muscio, A.L. Pisello, F. Rossi, M. Santamouris, A. Synnefa, N. Wong, M. Zinzi, Local climate change and urban heat island mitigation techniques – the state of the art, J. Civ. Eng. Manag. 22 (1) (2016) 1–16, <https://doi.org/10.3846/13923730.2015.1111934>.
- [5] A. Shwartz, A. Turbé, L. Simon, R. Julliard, Enhancing urban biodiversity and its influence on city-dwellers: an experiment, Biol. Conserv. 171 (2014) 82–90, <https://doi.org/10.1016/j.biocon.2014.01.009>.
- [6] K.A. Gray, M.E. Finster, The Urban Heat Island, Photochemical Smog, and Chicago: Local Features of the Problem and Solution, Northwestern University Tech. Rep., Atmospheric Pollution Prevention Division, EPA, 1999. <http://www.epa.gov/hir/resources/publications.html>.
- [7] C. Cartalis, A. Synodinou, M. Proedrou, A. Tsangrasoulis, M. Santamouris, Modifications in energy demand in urban areas as a result of climate changes: an assessment for the Southeast Mediterranean region, Energy Convers. Manag. 42 (14) (2001) 1647–1656, [https://doi.org/10.1016/S0196-8904\(00\)00156-4](https://doi.org/10.1016/S0196-8904(00)00156-4).
- [8] S. Hassid, M. Santamouris, M. Papanikolaou, A. Linardi, N. Klitsikas, C. Georgakis, The effect of the Athens heat island on air conditioning load, Energy Build. 32 (2000) 131–141, [https://doi.org/10.1016/S0378-7788\(99\)00045-6](https://doi.org/10.1016/S0378-7788(99)00045-6).
- [9] M. Santamouris, D. Kolokotsa, On the impact of urban overheating and extreme climatic conditions on housing, energy, comfort and environmental quality of vulnerable population in Europe, Energy Build. 98 (2015) 125–133, <https://doi.org/10.1016/j.enbuild.2014.08.050>.

- [10] J. Paravantis, M. Santamouris, C. Cartalis, C. Efthymiou, N. Kontoulis, Mortality associated with high ambient temperatures, heatwaves, and the urban heat island in athens, Greece, *Sustainability* 9 (2017) 606, 10.3390/su9040606.
- [11] The Multifunctionality of Green Infrastructure, Directorate-General for the Environment, March 2012. European Commission.
- [12] J. Coma, C. Solé, A. Castell, L.F. Cabeza, New green facades as passive systems for energy savings on buildings, *Energy Proc.* 57 (2014) 1851–1859, 10.1016/j.egypro.2014.10.049.
- [13] G. Pérez, J. Coma, I. Martorell, L.F. Cabeza, Vertical Greenery Systems (VGS) for energy saving in buildings: a review, *Appl. Energy* 88 (12) (2011) 4854–4859, 10.1016/j.rser.2014.07.055.
- [14] T. Safikhani, A.M. Abdullah, D.R. Ossen, M. Baharvand, A review of energy characteristic of vertical greenery systems, *Renewable Sustainable Energy Rev.* 40 (2014) 450–462, 10.1016/j.rser.2014.07.166.
- [15] R.C. Feitosa, S.J. Wilkinson, Attenuating heat stress through green roof and green wall retrofit, *Build. Environ.* 140 (2018) 11–22, 10.1016/j.buildenv.2018.05.034.
- [16] E. Fischer, M. Detommaso, F. Martinico, F. Nocera, V. Costanzo, A risk index for assessing heat stress mitigation strategies. An application in the Mediterranean context, *J. Clean. Prod.* 346 (2022), 131210. <https://doi.org/10.1016/j.jclepro.2022.131210>.
- [17] M. Detommaso, V. Costanzo, F. Nocera, Application of weather data morphing for calibration of urban ENVI-met microclimate models. Results and critical issues, *Urban Clim.* 38 (2021), 100895, <https://doi.org/10.1016/j.ulclim.2021.100895>.
- [18] M. Detommaso, A. Gagliano, L. Marletta, F. Nocera, Sustainable urban greening and cooling strategies for thermal comfort at pedestrian level, *Sustainability* 13 (2021) 3138, <https://doi.org/10.3390/su13063138>.
- [19] V. Oquendo-Di Cosola, F. Olivieri, L. Ruiz-García, A systematic review of the impact of green walls on urban comfort: temperature reduction and noise attenuation, *Renewable Sustainable Energy Rev.* 162 (2022), 112463, <https://doi.org/10.1016/j.rser.2022.112463>.
- [20] H. Gatringer, A. Claret, M. Radtke, J. Kissler, A. Zraunig, I. Rodriguez-Roda, G. Buttiglieri, Novel vertical ecosystem for sustainable water treatment and reuse in tourist resorts, *Int. J. Sustain. Dev. Plann.* 11 (2016) 263–274, <https://doi.org/10.2495/SDP-V11-N3-263-274>.
- [21] P. Wang, Y.H. Wong, C.Y. Tan, S. Li, W.T. Chong, Vertical greening systems: technological benefits, progresses and prospects, *Sustainability* 14 (2022), 12997, <https://doi.org/10.3390/su142012997>.
- [22] M.N. Assimakopoulos, R.F. De Masi, F. de Rossi, D. Papadaki, S. Ruggiero, GreenWall design approach towards energy performance and indoor comfort improvement: a case study in athens, *Sustainability* 12 (2020) 3772, <https://doi.org/10.3390/su12093772>.
- [23] I. Sosorova, Green facades and living walls: vertical vegetation as a construction material to reduce building cooling loads, in: *Eco-Efficient Materials for Mitigating Building Cooling Needs: Design, Properties and Applications*, Woodhead Publishing, Sawston UK, 2015, pp. 127–153.
- [24] M. Manso, J. Castro-Gomes, Green wall systems: a review of their characteristics, *Renewable Sustainable Energy Rev.* 41 (2015) 863–871, <https://doi.org/10.1016/j.rser.2014.07.203>.
- [25] R.A. Bustami, M. Belusko, J. Ward, S. Beecham, Vertical greenery systems: a systematic review of research trends, *Build. Environ.* 146 (2018) 226–237, <https://doi.org/10.1016/j.buildenv.2018.09.045>.
- [26] M. Radi, M. Brković Dodig, T. Auer, Green facades and living walls—a review establishing the classification of construction types and mapping the benefits, *Sustainability* 11 (2019) 4579, <https://doi.org/10.3390/su11174579>.
- [27] M. Kohler, Green facades – a view back and some visions, *Urban Ecosyst.* 11 (2008) 423–426, <https://doi.org/10.1007/s11252-008-0063-x>.
- [28] M. Rakhsandehroo, M. Yusof, M. Johari, M. Deghati Najd, Green façade (vertical greening): benefits and threats, *Appl. Mech. Mater.* 747 (2015) 12–15. <https://doi.org/10.4028/www.scientific.net/AMM.747.12>.
- [29] B. Riley, The state of the art of living walls: lessons learned, *Build. Environ.* 114 (2017) 219–232, <https://doi.org/10.1016/j.buildenv.2016.12.016>.
- [30] Shaimaa Seyam, The impact of greenery systems on building energy: systematic review, *J. Build. Eng.* 26 (2019), 100887, <https://doi.org/10.1016/j.jobe.2019.100887>.
- [31] M. Ottelé, K. Perini, Comparative experimental approach to investigate the thermal behaviour of vertical greened façades of buildings, *Ecol. Eng.* 108 (2017) 152–161, <https://doi.org/10.1016/j.ecoleng.2017.08.016>.
- [32] K. Perini, F. Bazzocchi, L. Croci, A. Magliocco, E. Cattaneo, The use of vertical greening systems to reduce the energy demand for air conditioning. Field monitoring in Mediterranean climate, *Energy Build.* 143 (2017) 35–42, <https://doi.org/10.1016/j.buildenv.2017.03.036>.
- [33] A.M. Hunter, N.S.G. Williams, J.P. Rayner, L. Aye, D. Hes, S.J. Livesley, Quantifying the thermal performance of green facades: a critical review, *Ecol. Eng.* 63 (2014) 102–113, <https://doi.org/10.1016/j.ecoleng.2013.12.021>.
- [34] T. Sternberg, Evaluating the role of ivy (Hereda helix) in moderating wall surface microclimates and contributing to the bioprotection of historic buildings, *Build. Environ.* 46 (2011) 293–297, <https://doi.org/10.1016/j.buildenv.2010.07.017>.
- [35] G. Vox, L. Blanco, E. Schettini, Green façades to control wall surface temperature in buildings, *Build. Environ.* 129 (2018) 154–166, <https://doi.org/10.1016/j.buildenv.2017.12.002>.
- [36] S. Flores Larsen, C. Filippin, G. Lesino, Modeling double skin green facades with traditional thermal simulation software, *Sol. Energy* 121 (2015) 56–67, <https://doi.org/10.1016/j.solener.2015.08.033>.
- [37] K.W.D.K.C. Dahanayake, C.L. Chow, Studying the potential of energy saving through vertical greenery systems: using EnergyPlus simulation program, *Energy Build.* 138 (2017) 47–59, <https://doi.org/10.1016/j.buildenv.2016.12.002>.
- [38] G. Perez, J. Coma, S. Sol, L.F. Cabeza, Green facade for energy savings in buildings: the influence of leaf area index and façade orientation on the shadow effect, *Appl. Energy* 187 (2017) 424–437, <https://doi.org/10.1016/j.apenergy.2016.11.055>.
- [39] C.A. Campiotti, L. Gatti, A. Campiotti, L. Consorti, P. De Rossi, C. Bibbiani, R. Muleo, A. Latini, Vertical greenery as natural tool for improving energy efficiency of buildings, *Horticulturae* 8 (2022) 526, <https://doi.org/10.3390/horticulturae8060526>.
- [40] N. Banti, C. Ciacci, V. Di Naso, F. Bazzocchi, Green walls as retrofitting measure: influence on energy performance of existing industrial buildings in Central Italy, *Buildings* 13 (2023) 369, <https://doi.org/10.3390/buildings13020369>.
- [41] L. Zhang, Z. Deng, L. Liang, Y. Zhang, Q. Meng, J. Wang, M. Santamouris, Thermal behavior of a vertical green facade and its impact on the indoor and outdoor thermal environment, *Energy Build.* 204 (2019), 109502, <https://doi.org/10.1016/j.enbuild.2019.109502>.
- [42] Y. Peng, Z. Huang, Y. Yang, P. Wang, C. Hou, Experimental investigation on the effect of vertical greening facade on the indoor thermal environment: a case study of dujiangyan city, sichuan province, *Earth and Environmental Science* 330 (2019), 032068, <https://doi.org/10.1088/1755-1315/330/3/032068>.
- [43] G. Kokogiannakis, J. Darkwa, S. Badeka, L. Yilin, Experimental comparison of green facades with outdoor test cells during a hot humid season, *Energy Build.* 185 (2019) 196–209, <https://doi.org/10.1016/j.enbuild.2018.12.038>.
- [44] P.A. Nguyen, R. Bokel, A.V.D. Dobbelsteen, Effects of a vertical green façade on the thermal performance and cooling demand. A case study of a tube house in vietnam, *J. Facade Des. Eng.* 7 (2) (2019) 44–63, <https://doi.org/10.7480/jfde.2019.2.3819>.
- [45] A. Ahmed Freewan, M. Ned'a Jaradat, A. Ikrima Amaireh, Optimizing shading and thermal performances of vertical green wall on buildings in a hot arid region, *Buildings* 12 (2022) 216, <https://doi.org/10.3390/buildings12020216>.
- [46] R. Djedjig, E. Bozonnet, R. Belarbi, Analysis of thermal effects of vegetated envelopes: integration of a validated model in a building energy simulation program, *Energy Build.* 86 (2015) 93–103, <https://doi.org/10.1016/j.enbuild.2014.09.057>.
- [47] I. Sosorova, M. Angulo, P. Bahrami, B. Stephens, A model of vegetated exterior façades for evaluation of wall thermal performance, *Build. Environ.* 67 (2013) 1–13.
- [48] <https://app.weathercloud.net/d8970100775#evolution>.
- [49] ISO 7726, *Ergonomics of the Thermal Environment — Instruments for Measuring Physical Quantities*, 1998.
- [50] Y. Zhang, L. Zhang, Q. Meng, Dynamic heat transfer model of vertical green façades and its co-simulation with a building energy modelling program in hot-summer/warm-winter zones, *J. Build. Eng.* 58 (2022), 105008, <https://doi.org/10.1016/j.jobe.2022.105008>.
- [51] W.J. Stec, A.H.C. Van Paassen, A. Maziarz, Modelling the double skin façade with plants, *Energy Build.* 37 (2005) 419–427, <https://doi.org/10.1016/j.enbuild.2004.08.008>.
- [52] K.J. Kontoleon, E.A. Eumorfopoulou, The effect of the orientation and proportion of a plant-covered wall layer on the thermal performance of a building zone, *Build. Environ.* 45 (2010) 1287–1303, <https://doi.org/10.1016/j.buildenv.2009.11.013>.
- [53] M. Scarpa, U. Mazzali, M. Peron, Modeling the energy performance of living walls: validation against field measurements in temperate climate, *Energy Build.* 79 (2014) 155–163, <https://doi.org/10.1016/j.enbuild.2014.04.014>.
- [54] K. Grabowiecki, A. Jaworski, T. Niewczas, A. Belleri, Green solutions – climbing vegetation impact on building – energy balance element, *Energy Proc.* 111 (2017) 377–386, <https://doi.org/10.1016/j.egypro.2017.03.199>.
- [55] Trnsys Component Type 9644 Green Façade – Vertical Foliage – VFC, CIM-mes Projekt Sp. z o.o. Warsaw, February 2022.
- [56] H.G. Jones, Plants and Microclimate. A Quantitative Approach to Environmental Plant Physiology, Cambridge University Press, Cambridge, 1992.
- [57] G.S. Campbell, J.M. Norman, An Introduction to Environmental Biophysics, Springer, New York, 1998.
- [58] S.C. Kaushik, R. Kumar, Performance evaluation of green roof and shading for thermal protection of buildings, *Build. Environ.* 40 (11) (2005) 1505–1511, <https://doi.org/10.1016/j.buildenv.2004.11.015>.
- [59] N.H. Wong, D.K.W. Cheong, H. Yan, J. Soh, C.L. Ong, A. Sia, The effect of rooftop garden on energy consumption of a commercial building in Singapore, *Energy Build.* 35 (2003) 353–364, [https://doi.org/10.1016/S0378-7788\(02\)00108-1](https://doi.org/10.1016/S0378-7788(02)00108-1).
- [60] J. Levitt, *Responses of Plants to Environmental Stresses: Chilling, Freezing, and High Temperature Stresses*, Academic Press, San Diego, 1980.
- [61] D.M. Gates, *Biophysical Ecology*, Dover Publicaitons, Inc, New York, 2003.
- [62] M. Kottek, J. Grieser, C. Beck, B. Rudolf, F. Rubel, World Map of the Köppen-Geiger climate classification updated, *Meteorol. Z.* 15 (3) (2006) 259–263, <https://doi.org/10.1127/0941-2948/2006/0130>.
- [63] UNI ISO 9869-1, *Isolamento termico – Elementi per l'edilizia – Misurazioni in situ della resistenza termica e della trasmittanza termica – Parte 1: Metodo del termoflussimetro*, 2015.
- [64] F. Convertino, G. Vox, E. Schettini, Evaluation of the cooling effect provided by a green façade as nature-based system for buildings, *Build. Environ.* 203 (2021), 108099, <https://doi.org/10.1016/j.buildenv.2021.108099>.
- [65] F. Convertino, E. Schettini, I. Blanco, C. Bibbiani, G. Vox, Effect of leaf area index on green facade thermal performance in buildings, *Sustainability* 14 (2022) 2966, <https://doi.org/10.3390/su14052966>.
- [66] TRNSYS 18 TRATransient SYstem Simulation Program, Volume 4, Mathematical Reference, (2018) 694–695.
- [67] M. Martin, P. Berdahl, Characteristics of infrared sky radiation in the United States, lawrence berkeley laboratory, university of California – berkeley, *Sol. Energy* 33 (3/4) (1984) 321–336.

- [68] TRNSYS 18 TRAnsient SYstem Simulation Program, Volume 4, Mathematical Reference, (2018), 484-487.
- [69] T. Kasuda, P.R. Archenbach, Earth temperature and thermal diffusivity at selected stations in the United States, *Build. Eng.* 71 (1) (1965).
- [70] Q. Chen, Q. Ding, X. Liu, Establishment and validation of solar radiation model for a living wall system, *Energy Build.* 195 (2019) 105–115, <https://doi.org/10.1016/j.enbuild.2019.05.005>.
- [71] F. Chianucci, J. Pisek, K. Raabe, L. Marchino, C. Ferrara, P. Corona, A dataset of leaf inclination angles for temperate and boreal broadleaf woody species, *Ann. For. Sci.* 75 (2018) 50, <https://doi.org/10.1007/s13595-018-0730-x>.
- [72] R. Pitman, M. Broadmeadow, Leaf Area, Biomass and Physiological Parameterization of Ground Vegetation of Low Land Oak Woodland, Surrey: Forest Research. An agency of the Forestry Commission, 2001.
- [73] S. Poddar, D. Park, S. Chang, Energy performance analysis of a dormitory building based on different orientations and seasonal variations of leaf area index, *Energy Efficiency* 10 (2017) 887–903.
- [74] G. Perez, J. Coma, M. Chafer, L.F. Cabeza, Seasonal influence of leaf area index (LAI) on the energy performance of a green façade, *Build. Environ.* 207 (2022), 108497, <https://doi.org/10.1016/j.buildenv.2021.108497>.
- [75] J. Mazur, Plants as natural anti-dust filters – preliminary research, *Environ. Eng. Technical transactions* 3/2018.
- [76] M. Ottelé, H.D. van Bohemen, A.L.A. Fraaij, Quantifying the deposition of particulate matter on climber vegetation on living walls, *Ecol. Eng.* 36 (2010) 154–162, <https://doi.org/10.1016/j.ecoleng.2009.02.007>.
- [77] A.M. Hunter, N.S.G. Williams, J.P. Rayner, L. Aye, D. Hes, Quantifying the thermal performance of green façades: a critical review, *Ecol. Eng.* 63 (2014) 102–113, <https://doi.org/10.1016/j.ecoleng.2013.12.021>.